American Mineralogist, Volume 74, pages 826–839, 1989

Vector representation of tourmaline compositions

Donald M. Burt
Department of Geology, Arizona State University, Tempe, Arizona 85287-1404, U.S.A.

Abstract

The vector method of representing mineral compositions, pioneered for the amphibole and mica groups, can be applied to the tourmaline group and improves upon traditional triangular representations. Formula information can be plotted directly on the diagrams or read directly from the diagrams, using ordinary graph paper or computer plotting routines. Each of the members of the tourmaline group can be derived from the composition of dravite, the Na-Mg-Al-$(OH)_4$ tourmaline. The first step is to "condense" down vectors of simple ionic exchange, such as $FeMg_{-1}$, $MnMg_{-1}$, $FeAl_{-1}$, $MnAl_{-1}$, $CrAl_{-1}$, VAl_{-1}, or $F(OH)_{-1}$. The major vectors are then $CaMg(NaAl)_{-1}$, which generates uvite, $LiAlMg_{-2}$, which generates elbaite and liddicoatite, and $AlO(MgOH)_{-1}$, which generates olenite and other tourmalines with variable OH contents. "Uncondensing" Fe generates schorl, feridravite, OH analogue of buergerite, and additional hypothetical Fe end-members and allows H gain or loss from tourmalines via the substitution $Fe^{3+}O(Fe^{2+}OH)_{-1}$, or $-H^0$ (atomic H). Na- or X-site vacancies are allowed by $[X]Al(NaMg)_{-1}$, minor octahedral Y-site vacancies by $[Y]Al_2Mg_{-3}$, Al for Si substitution by $MgSiAl_{-2}$, and octahedral cations in the Na,Ca site by $MgCa_{-1}$ or $Mg_2(NaAl)_{-1}$. These vectors can be combined to obtain numerous others of constant Na, Li, Mg, Fe, Ca, Al, Si, OH, and so on. These others are useful for drawing straight-line contours of element contents on vector diagrams and in drawing vector diagrams for degenerate subsystems (for example, Na-Al tourmalines, alkali-free tourmalines, and elbaites).

Introduction

In their introduction to the book, *Crystal Structures of Minerals,* Bragg et al. (1965, p. 24) cited the tourmaline group (along with micas and amphiboles) as a striking example of variable composition through complex isomorphous substitutions. Tourmaline is also of interest as the most common B mineral in granites, pegmatites, and a variety of other rock types. Thompson (1981, 1982; cf. Smith, 1959) successfully applied the concept of exchange vectors to the amphibole group, and Burt (in Černý and Burt, 1984, and Burt, 1989) applied it to the mica group and later to phyllosilicates in general (Burt, 1988). Application of the vector concept to the tourmaline group therefore seems appropriate, especially given recent reviews by Foit and Rosenberg (1977), Serdyuchenko (1978), Kuz'min et al. (1979), Povondra (1981), Feklichev et al. (1982), Werding and Schreyer (1984), Henry and Guidotti (1985), Dietrich (1985), Jolliff et al. (1986), and Deer et al. (1986).

The tourmaline formula, commonly given as $XY_3Z_6(BO_3)_3[Si_6O_{18}](OH,O,F)_4$, contains a total of 31 (O + OH + F) (e.g., Buerger et al., 1962). Table 1 shows most of the common ionic substitutions in this general formula (according to the above-cited reviews). For each ionic site a dashed line separates major substitutions (above), leading to named end-members, from lesser substitutions (below). The major substitutions occur in the X, Y, Z, and (OH) sites; there is also minor Al substitution for Si. The large X site is nine-coordinated and is generally filled by Na or Ca; the Y and Z sites are both six-coordinated, but the Y site tends to contain larger divalent cations (bonded to four O and two OH anions) and the Z site smaller trivalent cations (bonded to five O anions and one OH anion). There are two distinct OH sites, one with multiplicity 3. Only the unique OH site (surrounded by 3 Y-site octahedra) tends to be replaced by F (as in buergerite); the other three OH sites are more commonly replaced by O.

The named tourmaline end-members (with formulas modified from Fleischer, 1987) are listed in Table 2. "Tsilaisite," not listed, is also a "named end-member," although it is not a recognized mineral species. Its formula as generally (but not always: e.g., Slivko, 1961; Nuber and Schmetzer, 1984) given makes it the Mn analogue of schorl (not yet found in nature). The nine end-members in Table 2 are only a small fraction of those that could be written by combining the ions listed in Table 1. Many of these, including "tsilaisite," have been synthesized by Taylor and Terrell (1967) and some also by Tomisaka (1968). Of course, given the exchange-vector approach to describing complex ionic substitutions, the derivation and naming of end-members is arguably a fairly pointless exercise (Bragg et al., 1965, p. 22–23).

The key to the vector method is the concept of "ex-

0003–004X/89/0708–0826$02.00

TABLE 1. Typical ionic substitutions in the tourmaline structure.

$^{[9]}(X)$	Larger $^{[6]}(Y_3)$	Smaller $^{[6]}(Z_6)$	$(BO_3)_3$	$[Si_6O_{18}]$	$(OH)_3$	$(OH)_1$
Na^+	Mg^{2+}	Al^{3+}		Si^{4+}	$(OH)^-$	$(OH)^-$
Ca^{2+}	Fe^{2+}	Fe^{3+}		—	O^{2-}	F^-
—	Li^+	Cr^{3+}		Al^{3+}	—	—
[X]	Al^{3+}	Mg^{2+}*		B^{3+}?	F^-?	O^{2-}?
K^+	Fe^{3+}	—		P^{5+}?		Cl^-?
Mn^{2+}	—	Fe^{2+}		Fe^{2+}?		
Fe^{2+}	Mn^{2+}	Mn^{3+}				
Mg^{2+}	[Y]	V^{3+}				
	V^{3+}					
	Cr^{3+}					
	Ti^{4+}					

Note: [X] and [Y] designate X- and Y-site vacancies.
* Mg never fills more than ⅙ of the Z sites in uvite.

TABLE 2. Named tourmaline end-members

End-member	X	Y	Z	(O,OH,F)
Dravite	Na^+	Mg_3^{2+}	Al_6^{3+}	$(OH)_4$
Schorl	Na^+	Fe_3^{2+}	Al_6^{3+}	$(OH)_4$
Ferridravite	Na^+	Mg_3^{2+}	Fe_6^{3+}	$(OH)_4$
Chromdravite	Na^+	Mg_3^{2+}	Cr_6^{3+}	$(OH)_4$
Uvite	Ca^{2+}	Mg_3^{2+}	$Mg^{2+}Al_5^{3+}$	$(OH)_4$
Elbaite	Na^+	$Li_{1.5}^+Al_{1.5}^{3+}$	Al_6^{3+}	$(OH)_4$
Liddicoatite	Ca^{2+}	$Li_2^+Al^{3+}$	Al_6^{3+}	$(OH)_4$
Buergerite	Na^+	Fe_3^{3+}	Al_6^{3+}	O_3F
Olenite	Na^+	Al_3^{3+}	Al_6^{3+}	$O_3(OH)$

change operators" (Burt, 1974) or components that contain negative quantities of the elements to be exchanged (which is why I call them that; they perform the operation of exchange when added to a formula). A typical example, introduced in course lectures at Harvard University by J. B. Thompson, Jr., in the late 1960s, is $FeMg_{-1}$, which changes forsterite into fayalite (olivine) or dravite into schorl (tourmaline). Such exchange operators have both a direction (the direction opposite to $FeMg_{-1}$ is $MgFe_{-1}$) and a magnitude (that is, not only does the extent of Fe-Mg substitution vary, but also the operation must be applied twice to change the forsterite formula into that of fayalite, and three times to change the dravite formula into that of schorl); it is therefore logical to treat exchange operators as vectors. I reached this conclusion in 1981, shortly after J. B. Thompson, Jr. (following J. V. Smith, 1959), independently applied the concept to amphibole compositions. Of course, the chemical potentials of exchange operators ("exchange potentials") had been treated as vectors long before this date.

Exchange operators can involve exchange of cations [e.g., $MgCa_{-1}$], of anions [e.g., $F(OH)_{-1}$], or of some combination [e.g., $AlO(MgOH)_{-1}$, discussed below]. Each simple ion-exchange operator must be either acidic or basic in the electronic or Lewis (1938) sense (Burt, 1974), because no two ions share exactly the same electronic environment. Thus $MgCa_{-1}$ is acidic, and $CaMg_{-1}$ is basic. That concept is discussed elsewhere (Burt, 1979). The discussion is here confined to exchange operators used as vectors.

Diagrams involving exchange vectors are commonly anion conservative or cation conservative or both (cf. Brady and Stout, 1980). All of the diagrams given below conserve O or (O + F) (if H^+ in OH^- is considered a cation). A useful property is that the exchange vectors can be plotted manually on rectangular graph paper or by using standard computer x-y plotting routines (triangles are not needed). Straight-line contours can be drawn for the formula contents of individual ions, as illustrated in the figures. Extensions to the third dimension are straightforward.

In what follows, parts of the tourmaline formula that are not affected by the exchange operations are generally not labeled (i.e., they are understood to be present). Similarly, end-member compositions are referred to by the names of the corresponding minerals. "Derived from dravite," for example, means "derived from the composition or formula of dravite."

Application to common tourmalines

A vector defines an entire family of possible lines until it is attached to a starting point (or origin) to fix it in space. In composition space, this fixed starting point has been called the additive component (Thompson, 1982). For tourmalines, a suitable starting point is the composition of dravite, the Na-Mg-Al-$(OH)_4$ end-member, although any other end-member could be used. In this regard, Henry and Guidotti (1985), for example, observed that Mg/Fe and Na/Ca ratios in tourmaline are higher than in most coexisting phases. Schorl is then more common than dravite in pegmatites only because Mg has been depleted by fractional crystallization. This concept (Mg fractionation) also provides one of several possible explanations for the apparent lack of dravite-elbaite solid solutions in nature (see Dietrich, 1985, p. 83–84, for a review of the other explanations). All other tourmaline compositions can be derived from that of dravite by suitable exchange operations (Henry and Guidotti, 1985, mention the possibility). These operations are represented algebraically as exchange operators (a type of component) and graphically as exchange vectors.

As an example, Figure 1 shows the simultaneous operation of the two exchange vectors $MnMg_{-1}$ and $FeMg_{-1}$ on the composition of dravite. The vectors need not be drawn perpendicular nor of the same length, although doing so facilitates plotting. Subtracting the vertical vector from the horizontal yields the vector $MnFe_{-1}$, of slope -1. This is the slope of lines of constant Mg, just as slopes of lines of constant Mn are vertical and those of constant Fe horizontal (as marked on the vector diagram and shown by the labeled composition contours). For this special case of simple ionic substitutions, the vector approach offers no obvious advantage over using a normal barycentric triangle with Mg, Fe, and Mn at the corners. In fact, the vector approach yields such a triangle, which would be equilateral if the basis vectors are drawn 60° rather than 90° apart. Note, however, that on this trian-

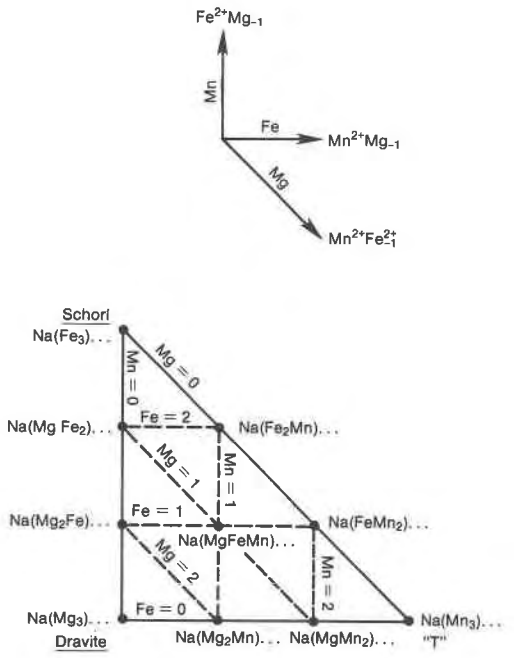

Fig. 1. Vector representation of tourmaline compositions derived from dravite by operation of the vectors $MnMg_{-1}$ (horizontal) and $FeMg_{-1}$ (vertical). Inset shows mutual relations of the basis and derived vectors. Remainder of the tourmaline formula is unchanged. "T" = manganoan end-member, sometimes designated "tsilaisite."

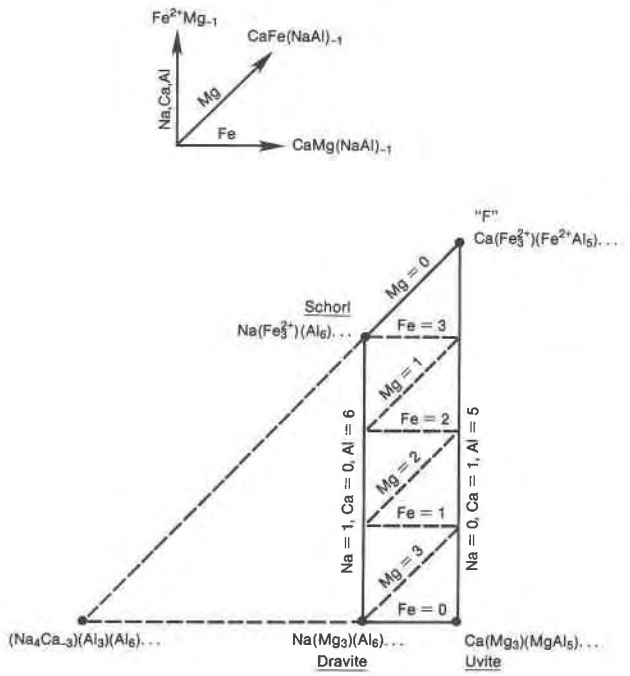

Fig. 2. Vector representation of tourmaline compositions derived from dravite by operation of the vectors $CaMg(NaAl)_{-1}$ (horizontal) and $FeMg_{-1}$ (vertical). "F" = hypothetical ferroan end-member.

gle, unlike on a mole fraction triangle (with plotted values running only between 0 and 1), formula contents can be read directly.

Figure 2 better demonstrates the advantages of the vector approach. The horizontal vector is the coupled substitution $CaMg(NaAl)_{-1}$, that, used once, changes dravite into uvite. The vertical vector is again $FeMg_{-1}$, that, if operated three times, changes dravite into schorl. On uvite, which has four Mg cations, it must be used four times to arrive at a hypothetical ferrous end-member "F," as shown. Lines of constant Ca, Na, or Al are vertical, and lines of constant Fe are horizontal (as labeled for the appropriate vectors). Adding the two vectors leads to a resultant, $CaFe(NaAl)_{-1}$, of slope +1. This vector is Mg-free and therefore defines the slope of lines of constant Mg. Note that lines of constant Mg are *not* parallel to lines of constant Fe in this type of representation, even though Mg and Fe substitute for each other. A conventional procedure would be to plot the diagram as mole fractions on a square, with Ca/(Na + Ca) as the horizontal axis and Fe/(Mg + Fe) as the vertical. Alternatively, the compositions might be plotted on a barycentric triangle, using as one corner the physically unattainable formula shown to the lower left. In contrast, the vector representation can be plotted directly from formulas, without the need for calculating mole fractions. It is, for this example, a quadrilateral, but not a square (and, in its physically attainable part, certainly not a triangle). As compared with barycentric representations, vector representations contain more information in a readily accessible form (that is, formula contents can be read directly from or plotted directly on the representation).

The Li-tourmalines elbaite and liddicoatite can similarly be derived from dravite and uvite by operation of the vector $LiAlMg_{-2}$, as shown in Figure 3. Because $LiAlMg_{-2}$ exchanges two Mg cations at a time, it only needs to be applied 1.5 times to change dravite into elbaite and twice to change uvite into liddicoatite. Consequently, the quadrilateral would be only half as high as that of Figure 2, except for scaling differences. Adding the horizontal and vertical vectors cancels Al in the resultant vector $CaLi(NaMg)_{-1}$ and thus gives the slope of lines of constant Al (+1); the vertical vector plus twice the horizontal cancels Mg in the resultant vector $Ca_2Li(Na_2Al)_{-1}$, or $CaLi_{0.5}(NaAl_{0.5})_{-1}$ and thus gives the slope of lines of constant Mg (+½). This vector is for obvious reasons called the "liddicoatite substitution" by Henry and Guidotti (1985, Table 2) and Henry and Dutrow (1987), although they list it as $CaLi(NaAl)_{-1}$.

In what follows, the mutual relations among other basis vectors (that is, those used to define the plane or space; the axes) and derived vectors (linear combinations of these) will be labeled in the figures, but not discussed in the text. In general, fictive end-member compositions,

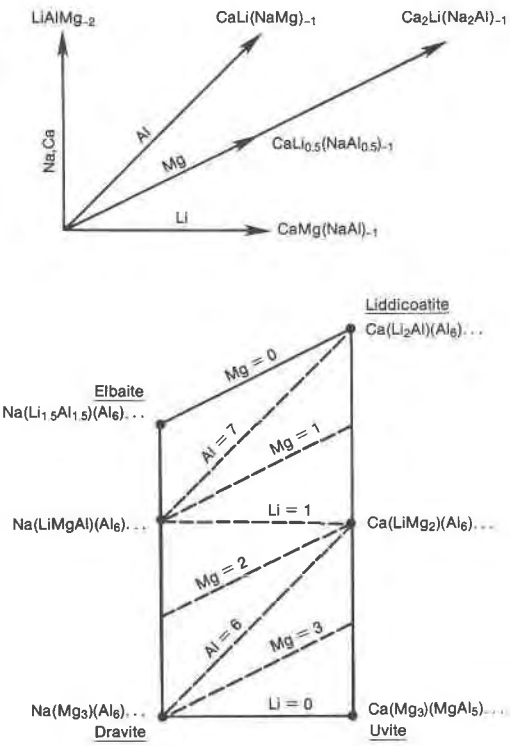

Fig. 3. Vector representation of tourmaline compositions derived from dravite by operation of the vectors CaMg(NaAl)$_{-1}$ (horizontal) and LiAlMg$_{-2}$ (vertical).

such as that to the left of Figure 2, will not be derived. These allow a triangular or pyramidal representation of compositions, an approach here discouraged.

The three vectors of Figures 2 and 3 are combined in Figure 4A. Figure 2 is the back face and Figure 3 the bottom face; no new end-members are generated because the Li-tourmalines contain no Mg. Neglecting variations in OH content and X-site vacancies, both discussed below, the compositions of most common tourmalines would fall in this volume. Figure 4B gives the basis and derived vectors used in Figure 4A. For example, the vector set labeled by "Li" doubly underlined (upper left of Fig. 4B) gives the vectors operating on a plane of constant Li (such as Fig. 2).

Many tourmalines contain Fe^{3+}, which can be accommodated by the vector $Fe^{3+}Al_{-1}$. One could draw a figure analogous to Figure 4, with $FeAl_{-1}$ instead of $FeMg_{-1}$ as the vertical vector. The elbaite corner would rise the most, 7.5 exchange units, to generate an unnamed Fe^{3+} analogue, the liddicoatite corner 7 units to generate another unnamed Fe^{3+} analogue, the dravite corner 6 units to generate ferridravite, and the uvite corner the least, 5 units, to generate a third unnamed Fe^{3+} analogue. These heights reflect the original Al contents of the formulas in Figure 3. Only ferridravite is a recognized mineral species, so that no figure is supplied. Operation of $CrAl_{-1}$ would analogously generate chromdravite plus three additional unnamed end-members; VAl_{-1} could likewise be used.

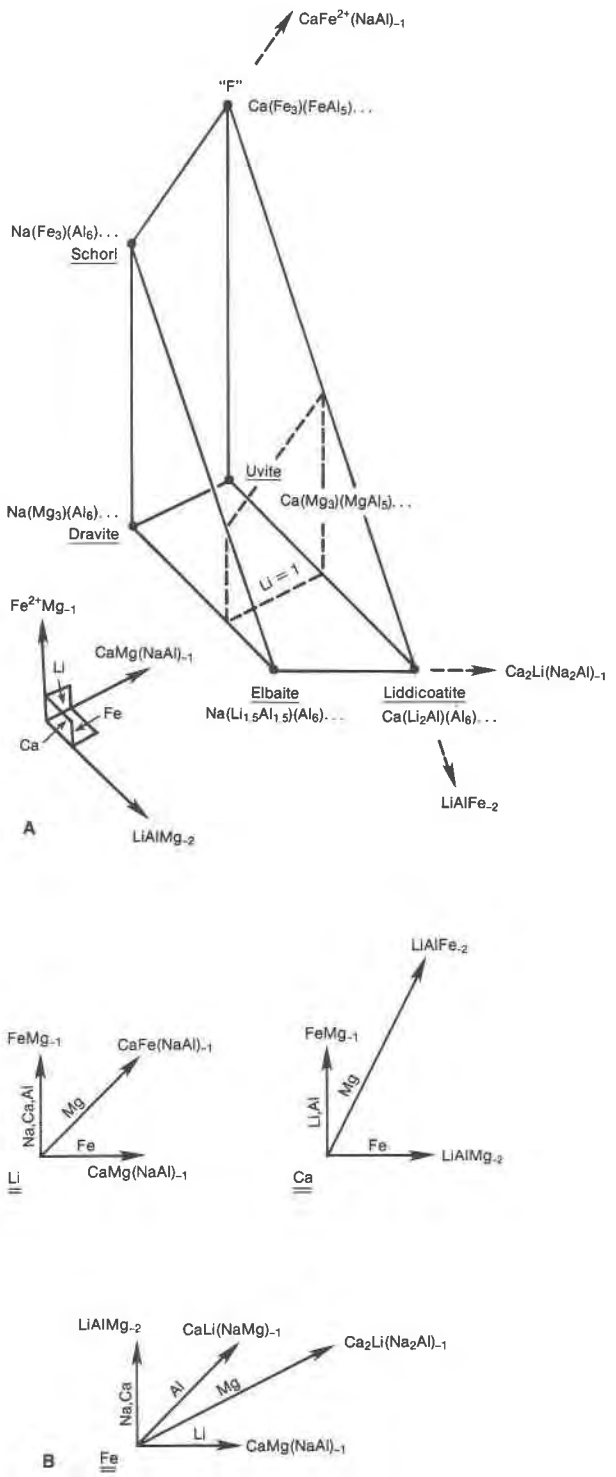

Fig. 4. Vector representations for common tourmalines. (**A**) Compositions derived from dravite by operation of the three vectors CaMg(NaAl)$_{-1}$ (upper right), LiAlMg$_{-2}$ (lower right), and FeMg$_{-1}$ (vertical). Neglecting O for OH substitutions and X-site vacancies, most tourmalines fall inside this volume. (**B**) Vector planes of constant Li, constant Ca (or Na), and constant Fe for Fig. 4A. Diagram shows basis and derived vectors, each labeled according to the ions that do not change along the vector.

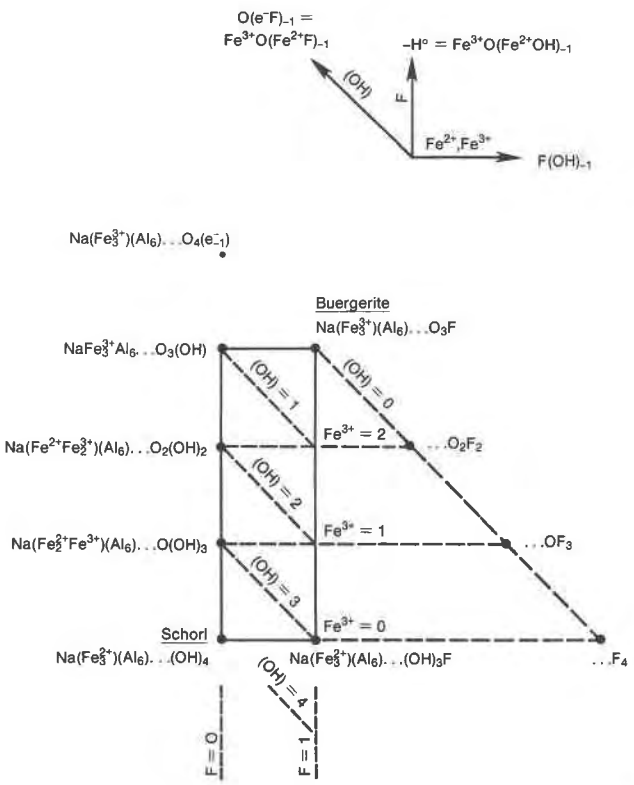

Fig. 5. Vector representation of the relation of schorl to buergerite. Diagram shows tourmaline compositions derived from schorl by operation of the vectors $F(OH)_{-1}$ (horizontal) and $Fe^{3+}O(Fe^{2+}OH)_{-1}$ (vertical), equivalent to $Fe^{3+}(Fe^{2+}H^{+})_{-1}$ or to minus H^0 (atomic H) or to loss of $\frac{1}{2}H_2$. Only one of the four hydroxyls in the tourmaline formula is readily replaced by F.

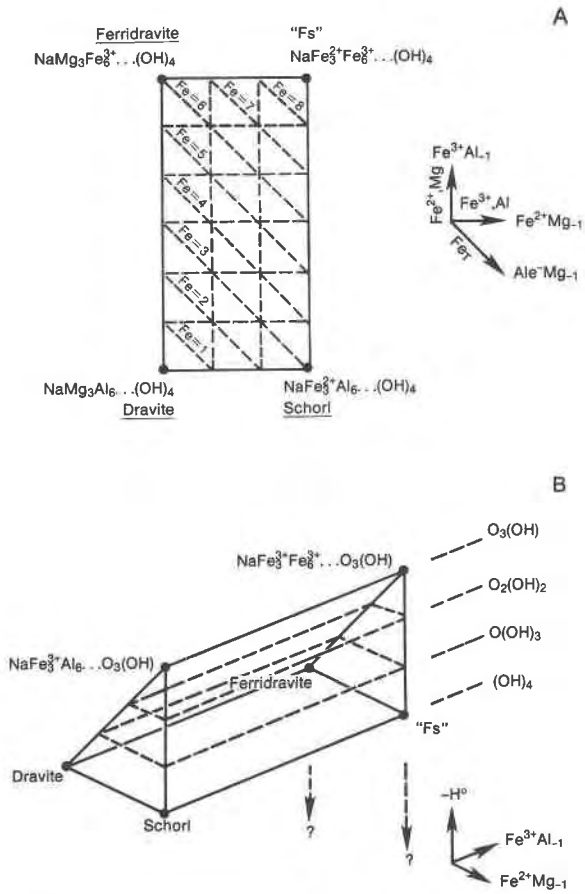

Fig. 6. Vector representation of tourmaline compositions derived from dravite by Fe^{2+} and Fe^{3+} substitutions. (**A**) Reciprocal ternary rectangle with operation of $FeMg_{-1}$ (horizontal) and $FeAl_{-1}$ (vertical). "Fs" = hypothetical Fe^{2+}-Fe^{3+} end-member. (**B**) Tourmaline compositions derived from Fig. 6A by loss of H^0 and oxidation of Fe^{2+} to Fe^{3+} (vertical). Downward arrows with question marks indicate the possibility of tourmaline with OH > 4.

Iron, fluorine, and variable hydroxyl

If Fe^{2+} and Fe^{3+} occur in the same tourmaline, it becomes easy to vary the hydroxyl content (cf. the classic papers on the same phenomenon in the micas by Eugster and Wones, 1962, and Wones and Eugster, 1965). This occurs via the coupled substitution $Fe^{3+}O(Fe^{2+}OH)_{-1}$, which simplifies to $-H^0$ (minus atomic H). In other words, a hydroxylated Fe^{2+} mineral, if heated in a vacuum or an oxidizing atmosphere, can change into a dehydrogenated Fe^{3+} analogue ("oxy-phase"), simply by loss of H from the OH groups. In principle, this should happen readily, and reversibly, because only migration of electrons and protons is involved. (By analogy, the same phenomenon should occur in tourmalines containing both Mn^{2+} and Mn^{3+}.) This situation contrasts with that for the analogous Mg-Al substitution, $AlO(MgOH)_{-1}$ (discussed below), which can only occur while the mineral is crystallizing.

The influence of the vector $Fe^{3+}O(Fe^{2+}OH)_{-1}$ on the composition of schorl is shown in Figure 5, for which the horizontal vector is $F(OH)_{-1}$. Only one of the four OH positions in tourmaline is easily replaced by F, as mentioned in the introduction (e.g., Němec, 1968, found consistently much less F in tourmaline than in coexisting micas, on a weight percentage basis), so that the F_4 composition is not observed. Operation of the two vectors together yields the composition of buergerite. The plotted composition with zero H and negative e^- could be called "electron-deficient oxybuergerite," analogous to a similar "proton-deficient oxyannite" composition plotted on a triangle by Wones and Eugster (1965, p. 1232). In a vector representation this "end-member" point serves no useful purpose; it is shown only for comparison with the Wones and Eugster study.

Simultaneous Fe^{2+} and Fe^{3+} substitutions in dravite are depicted in the reciprocal rectangle of Figure 6A; the Fe^{2+}-Fe^{3+} end-member, labeled "Fs," is unnamed. Note that the vector of constant Fe for this plane (slope -1) contains the electron, e^- (the result of subtracting Fe^{3+} from Fe^{2+}). Figure 6B shows possible oxy-tourmaline compositions derived from those of Figure 6A by subtracting H (oxidizing Fe^{2+}). The composition on the left (which also appears in Fig. 5) might be called "OH-buergerite" or "oxyschorl"; that on the right, "OH-ferribuergerite" or "oxy-ferrischorl" or some better term. Note that some

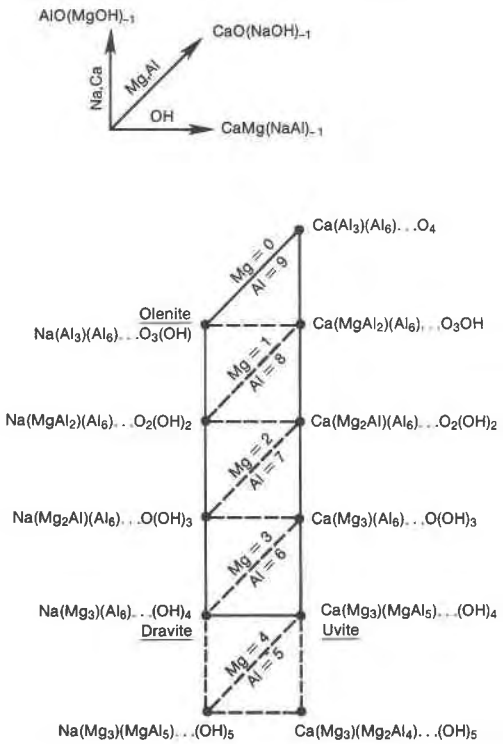

Fig. 7. Tourmaline compositions derived from dravite by operation of the vectors CaMg(NaAl)$_{-1}$ (horizontal) and AlO(MgOH)$_{-1}$ (vertical).

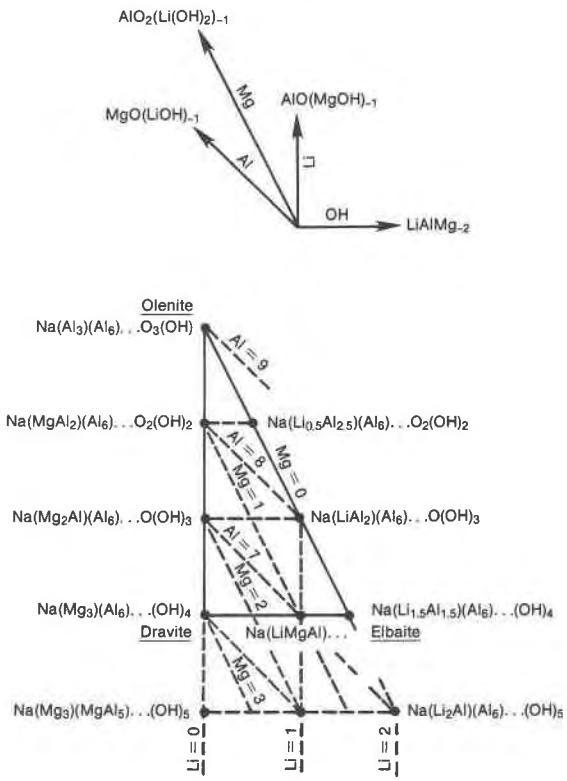

Fig. 8. Tourmaline compositions derived from dravite by operation of the vectors LiAlMg$_{-2}$ (horizontal) and AlO(MgOH)$_{-1}$ (vertical). Shows how Li and OH contents of elbaite are lowered by solid solution toward olenite.

tourmaline analyses have up to 5 (OH + F) (Foit and Rosenberg, 1977); possibly some of the Fe^{3+} in ferridravite or composition "Fs" in Figure 6 could be reduced under sufficient H_2 pressure, yielding compositions beneath the $(OH)_4$ plane (with more than four OH anions). This is indicated by the dashed downward-pointing arrows with question marks in Figure 6B.

Analogous Fe^{2+} and Fe^{3+} substitutions in uvite (not shown) would yield unnamed Fe^{2+}, Fe^{3+}, and Fe^{2+}-Fe^{3+} end-members. Schorl has four hydrogens and only three Fe^{2+} cations per formula unit, so that only three of the four hydrogens can be lost by oxidizing Fe. The Fe^{2+} analogue of uvite, on the other hand, has four Fe^{2+} cations and could theoretically lose all four of its hydrogens.

To simplify what follows, no separate mention is made of Fe^{2+} or Fe^{3+}; this is equivalent to "condensing down" the respective vectors FeMg$_{-1}$ and FeAl$_{-1}$; the same can be done for analogous vectors such as MnMg$_{-1}$, CrAl$_{-1}$, and VAl$_{-1}$. In other words, all divalent octahedral cations are treated as Mg, and all trivalent cations as Al. Similarly, (OH + F) is considered as equivalent to OH [condensing down F(OH)$_{-1}$].

Olenite and related compositions with variable hydroxyl

While hydroxyl (H^+ or H^0) gain or loss from Fe-bearing tourmalines should be fairly easy and could occur after crystallization, Fe-free tourmalines can also have a variable OH content (reviewed by Foit and Rosenberg, 1977) presumably inherited from the time of crystallization. The analogous substitution is AlO(MgOH)$_{-1}$, or Al(HMg)$_{-1}$, as shown in Figure 7. The end-member composition derived from dravite is olenite (Sokolov et al., 1986; earlier called "aluminobuergerite" by Foit and Rosenberg, 1975), with one hydroxyl; that derived from uvite is unnamed and has no hydroxyls. The above substitution—from its formula (equivalent to $\frac{1}{2}Al_2O_3 - MgO - \frac{1}{2}H_2O$)—would be favored in environments that are peraluminous, MgO (and FeO) deficient, and relatively anhydrous (high temperature), that is, in tourmalines crystallized in a differentiated peraluminous granitic melt or perhaps in a peraluminous granulite (cf. Grew, 1986). At the opposite extreme, tourmalines crystallized in low-temperature, hydrous, Al-poor and Mg-rich greenstones might have as many as five hydroxyls (see the bottom of Fig. 7).

Incidentally, Nuber and Schmetzer (1984) define a "tsilaisite" end-member of composition $Na(Mn_{1.5}Al_{1.5})Al_6(BO_3)_3Si_6O_{18}O_{1.5}(OH,F)_{2.5}$. On the Mn analogue of Figure 7 this "end-member" would lie half-way between the Mn analogue of dravite ("tsilaisite" as commonly defined) and olenite (consider also the Mn analogue of Fig. 8 for relations with elbaite). From a vector standpoint, then, there is no reason to favor the "end-member" composition chosen by Nuber and Schmetzer (1984).

The same substitution can influence the composition

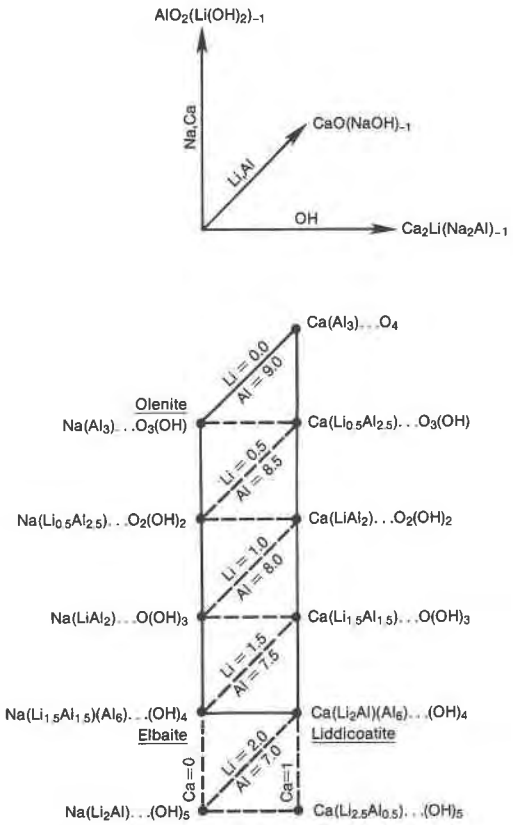

Fig. 9. Li-tourmaline compositions derived from elbaite by operation of the vectors $Ca_2Li(Na_2Al)_{-1}$ (horizontal) and $AlO_2(Li(OH)_2)_{-1}$ (vertical). The vertical vector lowers the Li and OH content of both Li-tourmalines.

of Li-tourmalines, as shown in Figure 8. Foit and Rosenberg (1977) noted that natural elbaites almost invariably contain fewer than the theoretical 1.5 Li cations but up to five OH anions. One way that Li deficiencies can occur is by solid solution toward olenite, as shown in Figure 8. In this case, the derived solid-solution vector is $AlO_2(Li(OH)_2)_{-1}$, so that the elbaite becomes OH deficient (other solid-solution vectors that do not lower OH are discussed below). The same vector can analogously lower the Li and OH content of liddicoatite, as shown in Figure 9 for mixed (Na,Ca)-tourmalines. All of these planes are faces on the condensed Li-Mg-Al-(O,OH) tourmaline volume depicted in Figure 10. This figure is analogous to Figure 4, except that Fe is condensed onto Mg (if Fe^{2+}) or Al (if Fe^{3+}) and F onto OH (so that schorl and ferridravite would plot with dravite, and buergerite with olenite), allowing the depiction of O and OH variations in only three dimensions. Figure 3 is the base, Figure 7 the back face, Figure 8 the left-side face, and Figure 9 the front face. Neglecting X-site vacancies, discussed below, most natural tourmaline compositions plot in this "condensed" volume.

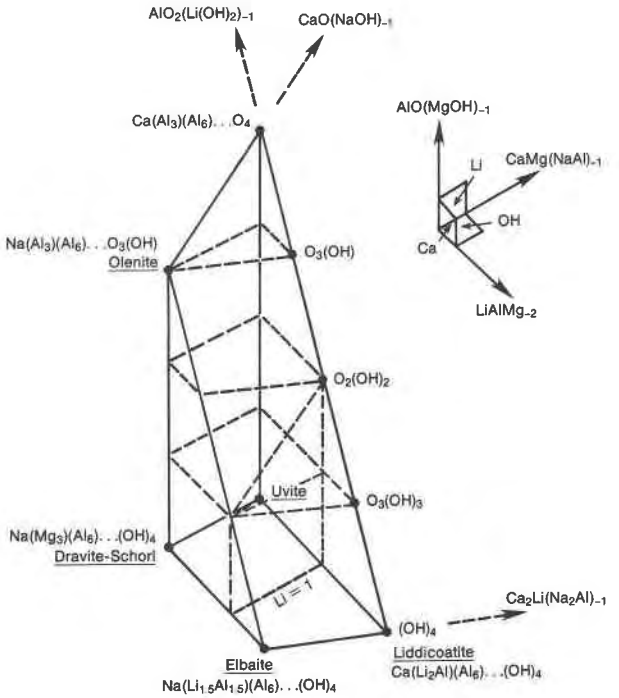

Fig. 10. Vector representation of "condensed" tourmaline composition space derived from dravite by operation of the three vectors $CaMg(NaAl)_{-1}$ (upper right), $LiAlMg_{-2}$ (lower right), and $AlO(MgOH)_{-1}$ (vertical). Neglecting X-site vacancies, most common tourmalines fall in this volume.

Octahedral vacancies

Foit and Rosenberg (1977) concluded that the Li contents of elbaites are also lowered by the presence of octahedral vacancies (assumed to be in the Y site). Figure 11 shows one way that this could occur, via solid solution toward a hypothetical dioctahedral end-member derived from schorl by operation of the vector $[Y]Al_2Mg_{-3}$ (the same one that changes phlogopite into muscovite, where the "Y" in the brackets indicates a Y-site vacancy). In contrast with the micas, such a dioctahedral composition, or anything close to it, is probably unstable (e.g., Foit and Rosenberg, 1977). The variable composition of elbaite is discussed further below.

Vacancies and octahedral cations in the X position

Better documented than vacancies in octahedral positions are vacancies in the X or (Na,Ca) position, designated [X]. Thus Rosenberg and Foit (1975, 1979) and Werding and Schreyer (1984) have been able to synthesize tourmalines without Na or Ca, of approximately the composition labeled "S" in Figure 12. The vector that brings this about is $[X]Al(NaMg)_{-1}$, similar to the vector leading to a deficiency of interlayer charge in tetrasilicic smectites and micas (e.g., Burt, 1988). A diagram very similar to Figure 12 is presented by Foit and Rosenberg

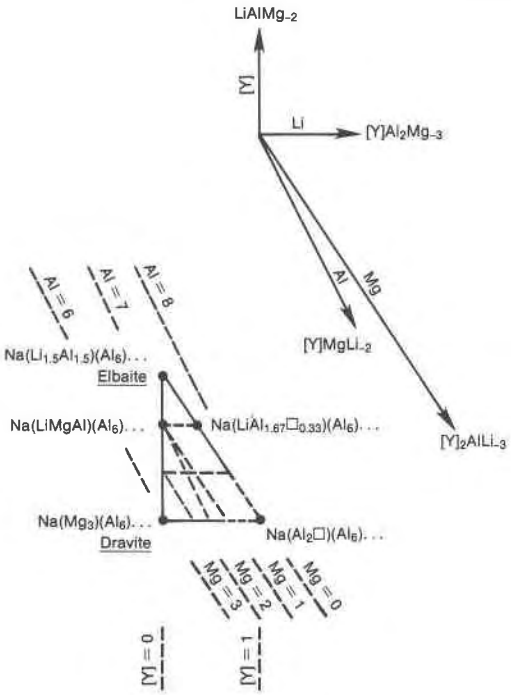

Fig. 11. Tourmaline compositions derived from dravite by operation of the vectors $[Y]Al_2Mg_{-3}$ (horizontal) and $LiAlMg_{-2}$ (vertical), where [Y] is a Y-site octahedral vacancy. Shows how octahedral vacancies could lower the Li content of elbaite.

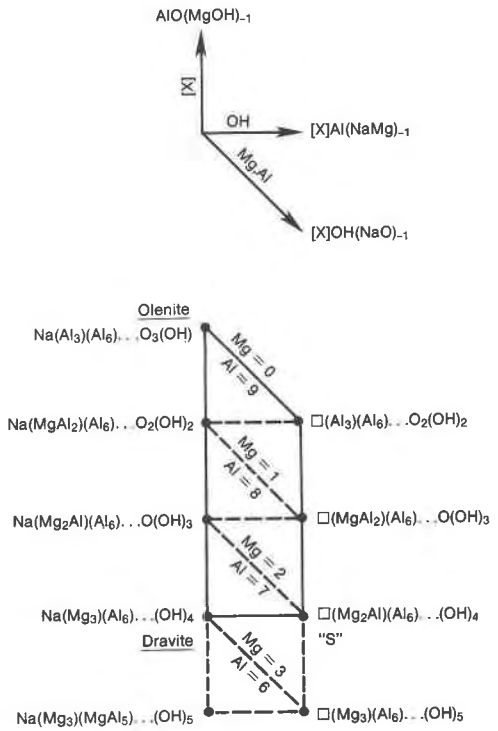

Fig. 12. Tourmaline compositions derived from dravite by operation of the vectors $[X]Al(NaMg)_{-1}$ (horizontal) and $AlO(MgOH)_{-1}$ (vertical), where [X] is an X-site vacancy. "S" is the approximate composition of a synthetic alkali-free tourmaline prepared by Rosenberg and Foit (1975) and Werding and Schreyer (1984).

(1977, Fig. 2) and by Povondra (1981, Figs. 3 and 4), although not in vector terms.

In case of alkali deficiency, X-position vacancies can be avoided by putting smaller cations such as Mg in this position, via a vector such as $Mg_2(NaAl)_{-1}$, or via derivatives such as $MgO(NaOH)_{-1}$ (Povondra, 1981; analogously, Mg instead of Na or Ca can provide interlayer charge in synthetic smectites: e.g., Velde, 1973). As shown in Figure 13, this leads to compositions such as "M," an Mg analogue of uvite, and related OH-deficient compositions (which were derived by Werding and Schreyer, 1984, Table 1, p. 1333). Werding and Schreyer reported that they were unable to synthesize any of these Mg endmember compositions (some of which were, however, reportedly synthesized by Rosenberg and Foit, 1975, 1985). Figure 13 is very similar to Figure 7, the difference being represented by the acidic operator $MgCa_{-1}$. At constant Al in the environment, Na depletion or leaching from tourmaline (as via acid solutions or reaction with wallrock) is likely to occur by some combination of Mg (or Ca) substitution and vacancy formation, such as along the vector $[X]MgNa_{-2}$ [a linear combination of $Mg_2(NaAl)_{-1}$ and $[X]Al(NaMg)_{-1}$]. Henry and Dutrow (1987) proposed a "Ca-deprotonation" substitution, $CaMgO([X]AlOH)_{-1}$, that leads to increased occupancy of the X site; this substitution can be shown to be a linear combination of vectors used above, namely $AlO(MgOH)_{-1} + CaMg(NaAl)_{-1} - [X]Al(NaMg)_{-1}$.

Vacancies in the X site can also lower the Li content of elbaite, as noted by Foit and Rosenberg (1977). Figure 14 illustrates this graphically; the Na-free composition would have only one Li. The effect on the dravite-elbaite series of simultaneous substituion of O for OH and of vacancies for Na are illustrated in Figure 15. Given that the Li content of elbaite can be lowered by solid solution toward olenite (O for OH substitution, shown in Figs. 8 and 15), octahedral vacancies (Fig. 11), or X-site vacancies (Figs. 14 and 15), perhaps it is amazing that natural elbaites contain any Li at all! Yet Al for Si substitution, discussed below, could further lower the content of Li.

Tschermak's and related substitutions

Most natural tourmalines grow under conditions of silica saturation and fairly constant alumina activity, so that there is little oppostunity for Al to substitute for Si. Synthetic tourmalines can be prepared over a much wider range of conditions and consequently might be expected to show a much more variable Si content (e.g., a (Na,Al)-tourmaline with only 4.22 Si cations prepared by Rosenberg et al., 1986). Such synthetic tourmalines provide the

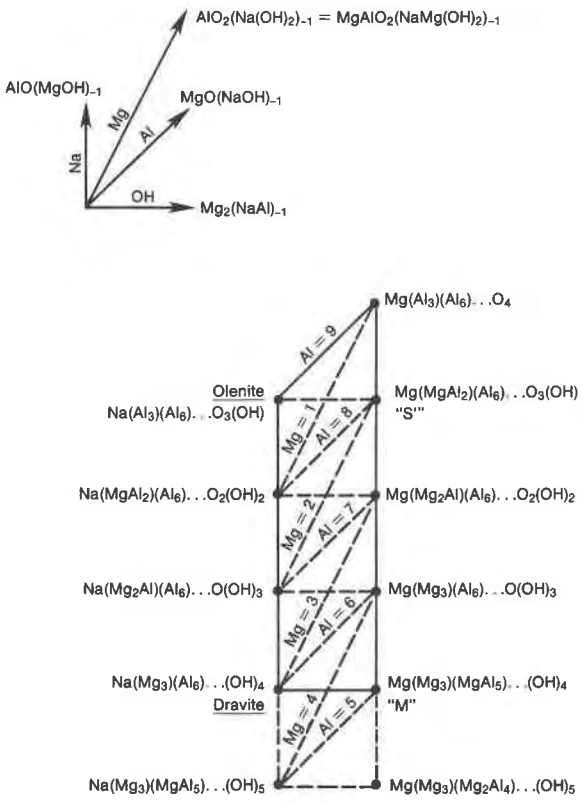

Fig. 13. Tourmaline compositions derived from dravite by operation of the vectors $Mg_2(NaAl)_{-1}$ (horizontal) and $AlO(MgOH)_{-1}$ (vertical). "M" corresponds to a magnesian analogue of uvite; "S" is a magnesian tourmaline synthesized by Rosenberg and Foit (1975).

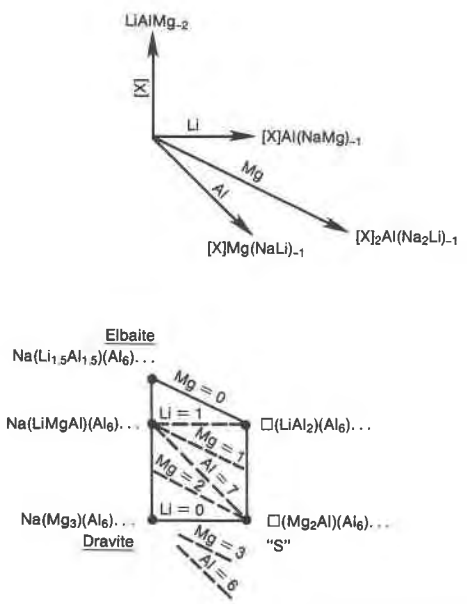

Fig. 14. Tourmaline compositions derived from dravite by operation of the vectors $[X]Al(NaMg)_{-1}$ (horizontal) and $LiAlMg_{-2}$ (vertical), where [X] is an X-site vacancy. Shows how X-site vacancies lower the Li content of elbaite. "S" is as in Fig. 12.

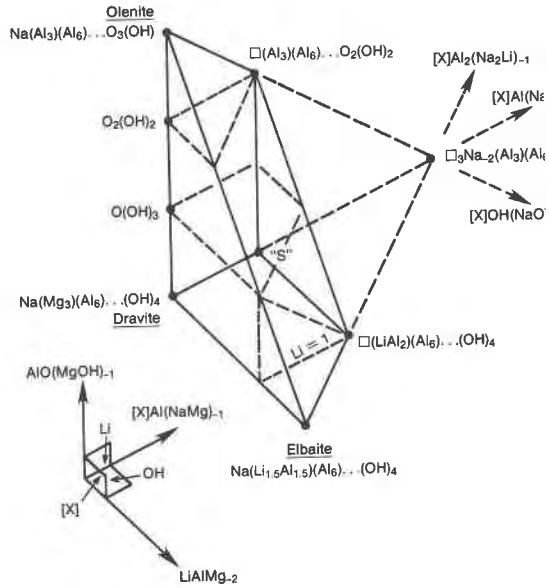

Fig. 15. Tourmaline compositions derived from dravite by operation of the three vectors $[X]Al(NaMg)_{-1}$ (upper right), $LiAlMg_{-2}$ (lower right), and $AlO(MgOH)_{-1}$ (vertical). "S" is as in Fig. 12.

justification for discussing a compositional variation that most published tourmaline analyses would show to be of negligible importance. (F. F. Foit et al., manuscript in preparation, have reported up to 0.46 [4]Al in tourmalines from a strongly peraluminous environment.)

Replacement of tetrahedral Si by Al in silicates is normally said to occur via the Tschermak's substitution, $Al_2(MgSi)_{-1}$ (cf. Thompson, 1979), although in hydroxyl-bearing phases one could just as readily use $SiO(AlOH)_{-1}$, derived by subtracting $Al_2(MgSi)_{-1}$ from $AlO(MgOH)_{-1}$, already used above (i.e., you could use one or the other, but not both). If you want Si contents to increase upward, use the "reverse Tschermak's" vector, $MgSiAl_{-2}$. Tourmaline compositions with octahedral defects in combination with the Tschermak's substitution are depicted in Figure 16. The Tschermak's substitution of dravite logically terminates at a Si content of 3, at which point the tourmaline has run out of Mg. Theoretically, it could also run in the other direction (to Si contents greater than 6), but only if some Si were placed in the smaller octahedral or Z position, as show by the labeled points. This is improbable at crustal pressures.

Planes analogous to Figure 16 are of major importance for chlorites, smectites, micas, and brittle micas (Burt, 1988), but the importance of Figure 16 for natural tourmaline compositions appears to be negligible. Inasmuch as lines of constant Mg and Al both have positive slopes, and MgO and Al_2O_3 activities are likely to be controlled by coexisting phases, one might predict that tourmalines with increasing octahedral defects would be more Si rich, just as muscovite is always more Si rich than coexisting phlogopite, but this remains conjecture.

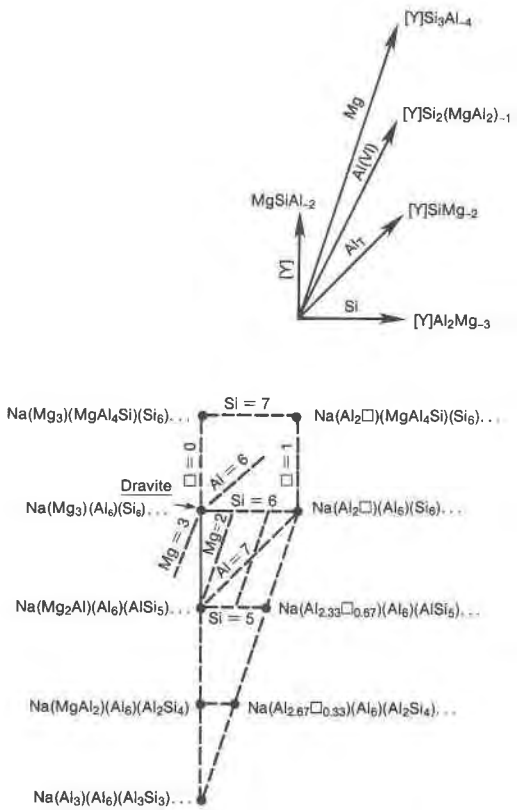

Fig. 16. Tourmaline compositions derived from dravite by operation of the vectors $[Y]Al_2Mg_{-3}$ (horizontal) and $MgSiAl_{-2}$ (vertical), where [Y] is an octahedral vacancy. This plane is of major importance for phyllosilicates, but of negligible importance for tourmaline.

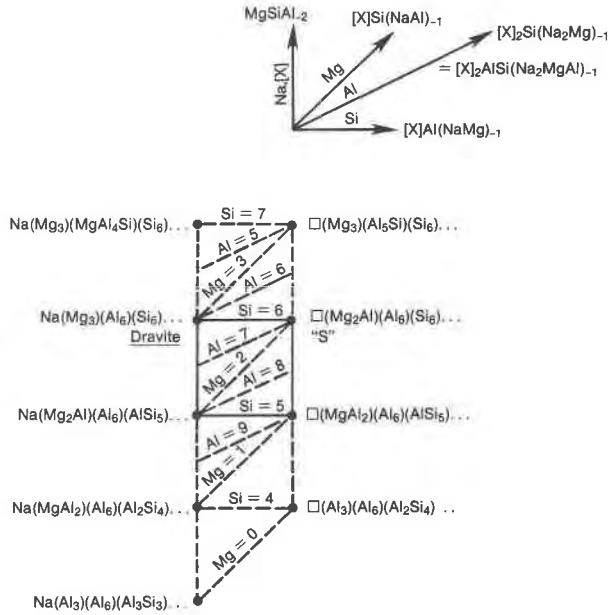

Fig. 17. Tourmaline compositions derived from dravite by operation of the vectors $[X]Al(NaMg)_{-1}$ (horizontal) and $MgSiAl_{-2}$ (vertical), where [X] is an X-site vacancy. "S" is as in Fig. 12.

An analogous plane for X-site vacancies (Fig. 17) yields lines of constant Mg and Al again having positive slopes; such slopes suggest that increasing X-site vacancies might correlate with increasing Si (a tendency confirmed by F. F. Foit et al. in the above-mentioned unpublished manuscript). For phyllosilicates, smectites lie on such a plane, intermediate between talc or pyrophyllite and micas (Burt, 1988).

A similar diagram for tourmalines with variable Ca and Si (not shown) would yield lines of constant Mg and Al having negative slopes, suggesting that increasing Ca might correlate with decreasing Si (this conjecture is again confirmed in the unpublished manuscript by F. F. Foit et al.).

Li-tourmalines from unusual environments might also vary in Si content. Figure 18 is a three-dimensional composition diagram for tourmalines with variable Li, Mg, Al, Si, and OH. Note how, with decreasing silica content, all three solid-solution series (dravite, olenite, and elbaite) converge to the same composition. Olenite does so by the vector $AlOH(SiO)_{-1}$, mentioned above. The vector for elbaite, $Al_3(LiSi_2)_{-1}$, also lowers its Li content.

Other interesting substitutions occur in the tourmaline group, particularly of minor octahedral Ti. As for the phyllosilicates (Burt, 1988), Ti could be introduced via the basis vector $TiMgAl_{-2}$, which only affects the Y (or Z) octahedral sites (using this basis vector does not necessarily imply that $TiMgAl_{-2}$ itself is an important substitution), but a graphical depiction is postponed pending

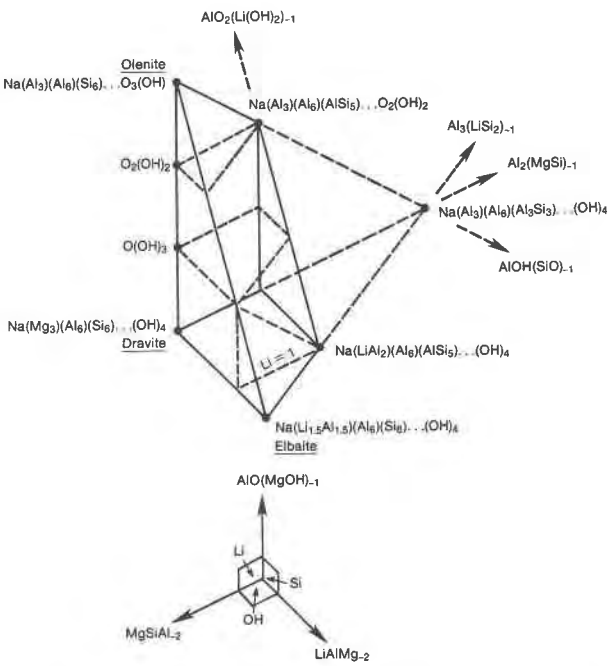

Fig. 18. Tourmaline compositions derived from dravite by operation of the three vectors $MgSiAl_{-2}$ (lower left), $LiAlMg_{-2}$ (lower right), and $AlO(MgOH)_{-1}$ (vertical).

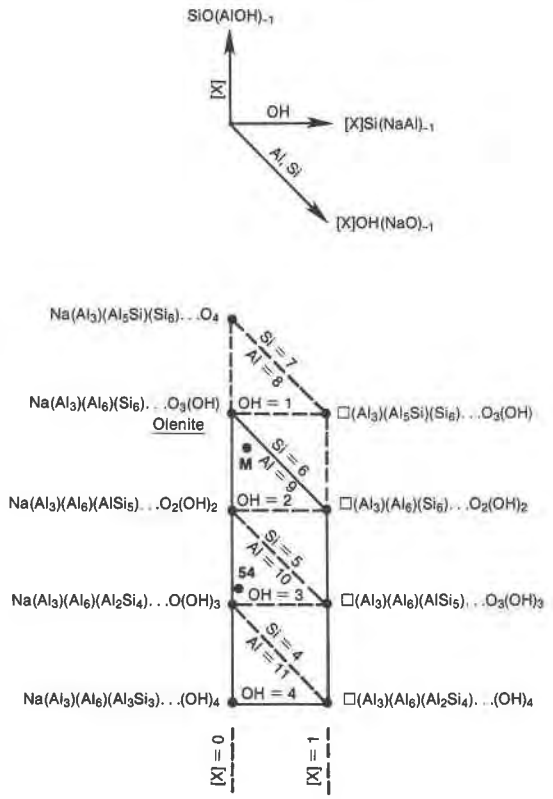

Fig. 19. Composition plane for (Na,Al)-tourmalines. Shows tourmaline compositions derived from olenite by operation of the vectors [X]Si(NaAl)$_{-1}$ (horizontal) and SiO(AlOH)$_{-1}$ (vertical), where [X] is an X-site vacancy. Points "54" and "M" are tourmalines synthesized by Rosenberg et al. (1986).

the discovery or synthesis of a Ti-rich tourmaline (none such are reported). The behavior of Ti in tourmaline is presumably analogous to its behavior in phyllosilicates (discussed in Burt, 1988).

Application to simpler systems

The above vector depictions apply to multicomponent natural tourmalines. Some experimental and natural tourmalines belong to simpler subsystems, however. For these, a different ("degenerate") set of exchange vectors might be appropriate. These vectors are linear combinations of the basis vectors used above.

(Na,Al)-tourmalines

Two tourmalines of reported compositions $([X]_{0.06}Na_{0.94})Al_3Al_6(Si_{4.22}Al_{1.78})(BO_3)_3O_{19.2}(OH)_{2.8}$ and $([X]_{0.24}Na_{0.76})Al_3Al_6(Si_{5.82}Al_{0.18})(BO_3)_3O_{20.6}(OH)_{1.4}$ were synthesized in the system Na_2O-Al_2O_3-B_2O_3-SiO_2-H_2O by Rosenberg et al. (1986). Their approximate compositions are points "54" and "M" in Figure 19, respectively. If necessary, a third vector, $[Y]Si_3Al_{-4}$, could have been added for octahedral vacancies (not reported and therefore not shown).

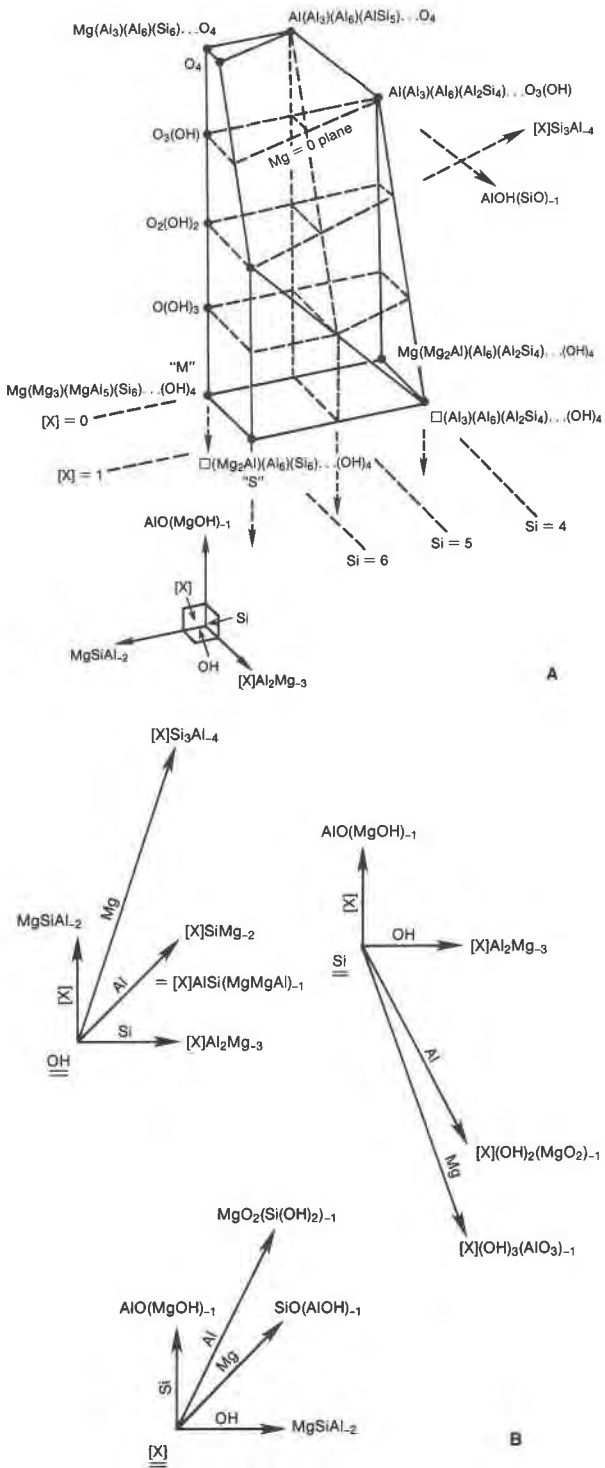

Fig. 20. Composition volume for alkali-free tourmalines. (**A**) Tourmaline compositions derived from "M" (magnesian analogue of uvite) by operation of the vectors [X]Al$_2$Mg$_{-3}$ (lower right), MgSiAl$_{-2}$ (lower left), and AlO(MgOH)$_{-1}$ (vertical), where [X] refers to an X-site vacancy. "S" is as in Fig. 12. Plane sloping toward the right front has Mg = 0. (**B**) Basis and derived vectors for planes of constant OH, Si, and [X] in Fig. 20A.

Alkali-free tourmalines

Alkali-free tourmalines are reported in the system MgO-Al_2O_3-B_2O_3-SiO_2-H_2O by Rosenberg and Foit (1975, 1979, 1985) and by Werding and Schreyer (1984). These authors attempted to project their compositions onto the triangle MgO-Al_2O_3-SiO_2; the volume of Figure 20A is more appropriate, inasmuch as it allows for X-site vacancies, the Tschermak's substitution, and O for OH substitution. The 10 experimental tourmaline compositions from Table 4 of Rosenberg and Foit (1985, p. 1222) could be plotted simply and directly in this figure but are not shown to avoid obscuring its basic features. Basis and derived vectors for Figure 20A (and for analogous figures involving other hydrous (Mg,Al)-silicates) are given in Figure 20B. Note that octahedral vacancies, [Y], could be substituted for X-site vacancies, [X], in these vectors for a gain in generality.

Elbaites

The theoretical Li content of elbaite (as generated from dravite by the vector $LiAlMg_{-2}$) is 1.5 per 31(O + OH + F). As mentioned above, Foit and Rosenberg (1977) noted that the analyzed Li contents are always lower and that OH + F contents can rise to 5 (instead of the theoretical 4). They hypothesized that Li could be lowered by (1) O for OH and Al for Li substitution [solid solution toward olenite via $AlO_2(Li(OH)_2)_{-1}$], lowering OH; (2) the introduction of octahedral Y-site vacancies (solid solution toward a dioctahedral end-member via $[Y]_2AlLi_{-3}$ as derived above, in which case they hypothesized the derivative substitution $[Y]OH(LiO)_{-1}$, which also substitutes OH for O, raising OH; or (3) Na- or X-site vacancies (solid solution toward a defect end-member via the substitution $[X]_2Al(Na_2Li)_{-1}$). These substitutions have been shown above individually and in pairs (e.g., Figs. 8, 11, and 14); Figure 21A shows them all together, and Figure 21B gives the basis and derived vectors used. The shaded plane satisfies the condition that Li be equal to a reduced value of 1.0; the sloping front face on the right side corresponds to "elbaites" with no Li whatever (and indicates potential confusion over "elbaite" vs. "olenite"). This is a solid-solution volume for elbaites; the positions of points inside it can be described in terms of any linearly independent set of three exchange vectors (not necessarily the ones used).

Given a fourth dimension, I could depict the further lowering of the Li content of elbaite caused by the Al for

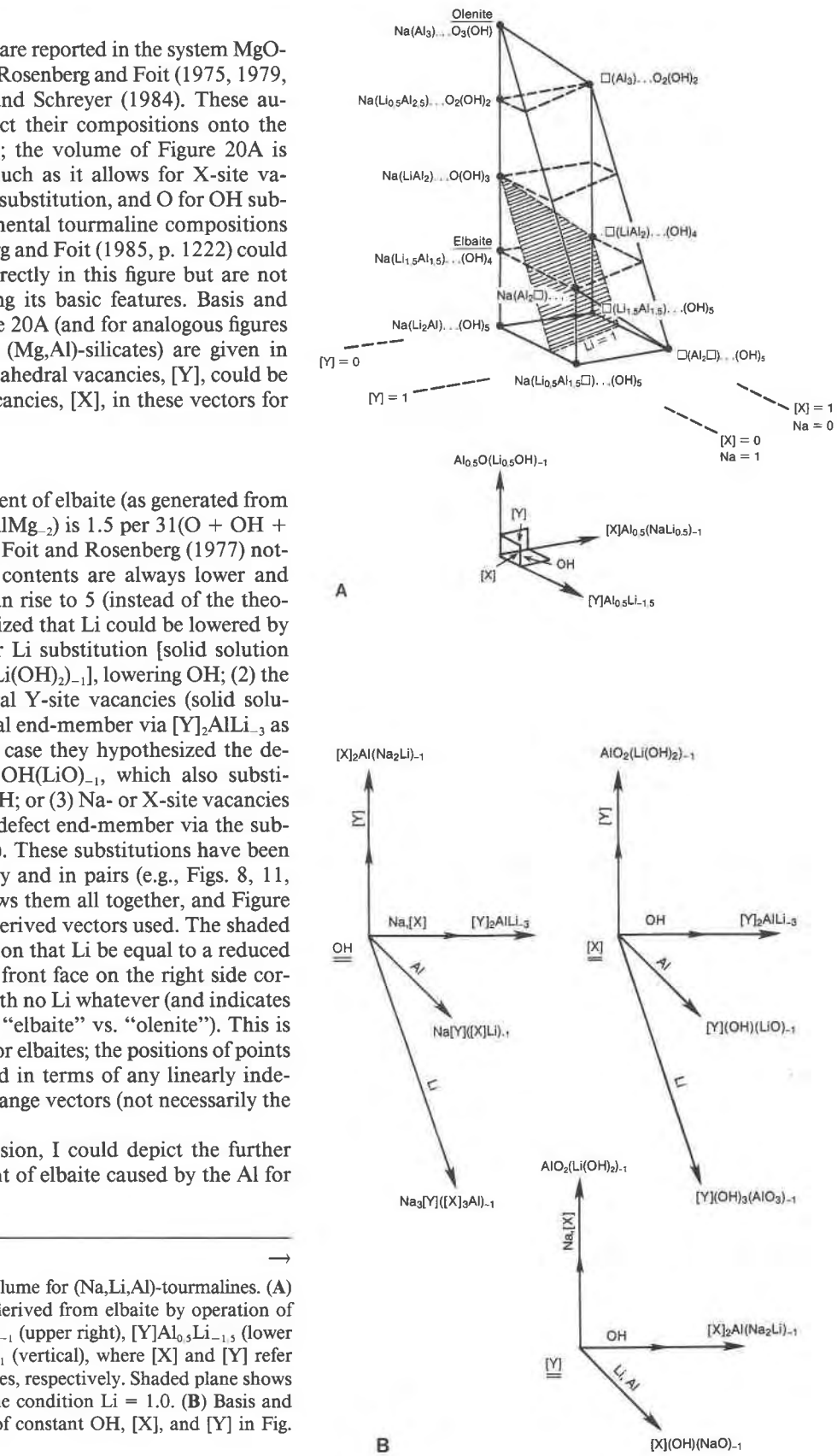

Fig. 21. Composition volume for (Na,Li,Al)-tourmalines. (**A**) Tourmaline compositions derived from elbaite by operation of the vectors $[X]Al_{0.5}(NaLi_{0.5})_{-1}$ (upper right), $[Y]Al_{0.5}Li_{-1.5}$ (lower right), and $Al_{0.5}O(Li_{0.5}OH)_{-1}$ (vertical), where [X] and [Y] refer to X-site and Y-site vacancies, respectively. Shaded plane shows compositions that satisfy the condition Li = 1.0. (**B**) Basis and derived vectors for planes of constant OH, [X], and [Y] in Fig. 21A.

Si substitution $Al_3(LiSi_2)_{-1}$, shown in Figure 18 (and not reported by Foit and Rosenberg, 1977). Alternatively, I could draw three diagrams for the other three combinations of the four vectors taken three at a time. However, perhaps the point is sufficiently made that trying to consider tourmaline compositions without using vectors is like primitive man trying to hunt without using spears or arrows.

Summary and conclusions

Vector representations on normal graph paper (instead of triangles) make possible the simple depiction of a wide range of possible tourmaline end-member compositions and solid solutions, starting from a single point. Starting from dravite, $FeMg_{-1}$ generates schorl and $FeAl_{-1}$ ferridravite (applying both yields a Fe^{2+}-Fe^{3+} analogue). Again from dravite, $CaMg(NaAl)_{-1}$ generates uvite, and with $FeMg_{-1}$ a Fe^{2+} analogue of uvite, with $FeAl_{-1}$ a Fe^{3+} analogue (with both a Fe^{2+}-Fe^{3+} analogue), and with $MgCa_{-1}$, a Mg analogue [which alternatively is obtained with $Mg_2(NaAl)_{-1}$]. From dravite, $LiAlMg_{-2}$ generates elbaite and, with $CaMg(NaAl)_{-1}$, liddicoatite. From dravite, $AlO(MgOH)_{-1}$ generates olenite; from schorl, its Fe^{3+}-Fe^{3+} analogue (equivalent to minus hydrogen) plus $F(OH)_{-1}$ generates buergerite.

Minor octahedral defects in tourmaline can be generated by $[Y]Al_2Mg_{-3}$ (as for micas); more important X-site defects via $[X]Al(NaMg)_{-1}$ (as for interlayer sites in micas). Variations in Si content can be generated by the Tschermak's vector $MgSiAl_{-2}$. Numerous other vectors can be derived by linear combination of those listed, and any linearly independent set would be valid for graphical representations or for describing actual solid-solution relations analytically. A different set of exchange vectors is especially appropriate for describing the compositional variations of compositionally restricted tourmalines, as demonstrated for (Na,Al)-tourmalines, alkali-free tourmalines, and elbaites.

Note that tourmaline end-members generated by the vector method need not be stable (e.g., those with octahedral vacancies), inasmuch as structural and other crystal-chemical factors are not considered. Instead, the vector method provides a simple graphical depiction of ionic charge restrictions on possible formulas. Note also that tourmaline is a multicomponent solid solution; consequently, its composition is not constrained to vary along a single vector, on a single plane, or in a single three-dimensional space. Vectors don't reduce the number of components; they are a different way of looking at components. On the other hand, most common tourmaline compositions probably fall in Figure 4 or (condensed) in Figure 10 (with some tendency for X-site vacancies as depicted in Fig. 15).

This is not the first place where the above conclusions have been stated in words (e.g., Henry and Guidotti, 1985); this paper demonstrates (1) how to draw the relevant vector diagrams, (2) how to relate the exchange vectors to each other, and (3) how to contour the diagrams for constant values of Na, Ca, Li, Fe, Mg, Al, Si, OH, and so on. The diagrams themselves thus constitute the major result of this study. Even so, there are numerous additional diagrams that could be drawn. Now that the method is demonstrated, I assign the rest for homework.

Acknowledgments

J. B. Thompson, Jr., first suggested to me the concept behind exchange operators and has inspired me to continue using them. I also am grateful to previous workers on coupled substitutions in the tourmaline group (F. F. Foit, P. E. Rosenberg, P. J. Dunn, P. Povondra, D. J. Henry, R. V. Dietrich, and many others) for making this paper a relatively easy one to write. Finally, I thank P. B. Leavens, D. London, F. F. Foit, Jr., E. S. Grew, and R. V. Dietrich for careful and thoughtful reviews and Deborah Barron for drafting the figures.

This work was performed while I was a Visiting Scientist at the Lunar and Planetary Institute, which is operated by the Universities Space Research Association under Contract No. NASW-4066 with the National Aeronautics and Space Administration. This paper is Lunar and Planetary Institute Contribution No. 703.

References cited

Brady, J.B., and Stout, J.H. (1980) Normalizations of thermodynamic properties and some implications for graphical and analytical problems in petrology. American Journal of Science, 180, 173–189.

Bragg, L., Claringbull, G.F., and Taylor, W.H. (1965) Crystal structures of minerals, 409 p. Cornell University Press, Ithaca, New York.

Buerger, M.J., Burnham, C.W., and Peacor, D.R. (1962) Assessment of the several crystal structures proposed for tourmaline. Acta Crystallographica, 15, 583–590.

Burt, D.M. (1974) Concepts of acidity and basicity in petrology—The exchange operator approach. Geological Society of America Abstracts with Programs, 6, 674–676.

——— (1979) Exchange operators, acids, and bases. In V.A. Zharikov, W.I. Fonarev, and S.P. Korikovskiy, Eds., Problems in physico-chemical petrology, vol. 2, p. 3–15. "Nauka" Press, Moscow (in Russian).

——— (1988) Vector representation of phyllosilicate compositions. Mineralogical Society of America Reviews in Mineralogy, 19, 561–599.

——— (1989) Vector representation of lithium and other mica compositions. In L.L. Perchuk, Ed., Advances in physical geochemistry (D.S. Korzhinskii memorial volume), in press. Springer-Verlag, New York.

Černý, P., and Burt, D.M. (1984) Paragenesis, crystallochemical characteristics, and geochemical evolution of micas in granitic pegmatites. Mineralogical Society of America Reviews in Mineralogy, 13, 257–297.

Deer, W.A., Howie, R.A., and Zussman, J. (1986) Rock-forming minerals, vol. 1B (2nd edition): Disilicates and ring silicates, 623 p. Longman Scientific, Essex, England.

Dietrich, R.V. (1985) The tourmaline group, 300 p. Van Nostrand Reinhold, New York.

Eugster, H.P., and Wones, D.R. (1962) Stability relations of the ferruginous biotite, annite. Journal of Petrology, 3, 82–125.

Feklichev, V.G., Ivanova, T.N., Cherepivskaya, G.E., and Nikitina, I.B. (1982) Study of composition-property relations in tourmaline-group minerals. Trudy Mineralogicheskogo Muzeya, Akademiya Nauk SSSR, 30, 154–168 (in Russian).

Fleischer, M. (1987) Glossary of mineral species (5th edition), 234 p. Mineralogical Record, Tucson, Arizona.

Foit, F.F., Jr., and Rosenberg, P.E. (1975) Aluminobuergerite, $Na_{1-x}Al_3Al_6B_3Si_6O_{27}O_{3-x}(OH)_{1+x}$, a new end-member of the tourmaline group (abs.). EOS, 56, 461.

——— (1977) Coupled substitutions in the tourmaline group. Contributions to Mineralogy and Petrology, 62, 109–127.

Grew, E.S. (1986) Petrogenesis of kornerupine at Waldheim (Sachsen), German Democratic Republic. Zeitschrift für geologischen Wissenschaften, 14, 525–558 (not seen; extracted from Mineralogical Abstracts, 38, 575, 1987).

Henry, D.J., and Dutrow, B.L. (1987) Ca-deprotonation in tourmaline

from aluminous metamorphic rocks. Geological Society of America Abstracts with Programs, 19, 700.

Henry, D.J., and Guidotti, C.V. (1985) Tourmaline as a petrogenetic indicator mineral: An example from the staurolite-grade metapelites of NW Maine. American Mineralogist, 70, 1–15.

Jolliff, B.L., Papike, J.J., and Shearer, C.K. (1986) Tourmaline as a recorder of pegmatite evolution: Bob Ingersoll pegmatite, Black Hills, South Dakota. American Mineralogist, 71, 472–500.

Kuz'min, V.I., Dobrovolskaya, N.V., and Solntseva, L.S. (1979) Tourmaline and its use in prospecting-evaluation work, 269 p. Moscow, "Nedra" Press (in Russian).

Lewis, G.N. (1938) Acids and bases. Journal of the Franklin Institute, 226, 293–313.

Němec, D. (1968) Fluorine in tourmalines. Contributions to Mineralogy and Petrology, 20, 235–243.

Nuber, B., and Schmetzer, K. (1984) Structural refinement of tsilaisite (manganese tourmaline). Neues Jahrbuch für Mineralogie Monatshefte, 301–304.

Povondra, P. (1981) The crystal chemistry of tourmalines of the schorl-dravite series. Acta Universitatis Carolinae–Geologica, no. 3, 223–264.

Rosenberg, P.E., and Foit, F.F., Jr (1975) Alkali-free tourmalines in the system MgO-Al_2O_3-SiO_2-H_2O-B_2O_3. Geological Society of America Abstracts with Programs, 7, 1250.

——— (1979) Synthesis and characterization of alkali-free tourmaline. American Mineralogist, 64, 180–186.

——— (1985) Tourmaline solid solutions in the system MgO-Al_2O_3-SiO_2-B_2O_3-H_2O. American Mineralogist, 70, 1217–1223.

Rosenberg, P.E., Foit, F.F., Jr., and Ekambaram, V. (1986) Synthesis and characterization of tourmaline in the system Na_2O-Al_2O_3-SiO_2-B_2O_3-H_2O. American Mineralogist, 71, 971–976.

Serdyuchenko, D.P. (1978) On the chemical constitution of tourmalines. In L.N. Ovchinnikov et al., Eds., Problemy Geologii Redkikh Elementov, p. 225–251. "Nauka" Press, Moscow (in Russian).

Slivko, M.N. (1961) Manganese tourmalines. International Geology Review, 3, 195–201 (translated from Mineralogicheskiy Sbornik, L'vov, no. 13, 139–148, 1959).

Smith, J.V. (1959) Graphical representation of amphibole compositions. American Mineralogist, 44, 437–440.

Sokolov, P.B., Groskaya, M.G., Gordienko, V.V., Petrova, M.G., Kretser, Yu.L., and Frank-Kamenitskiy, V.A. (1986) Olenite, $Na_{1-x}Al_3Al_6B_3Si_6O_{27}(O,OH)_4$, a new high-alumina mineral from the tourmaline group. Zapiski Vsesoyuznogo Mineralogicheskogo Obshchestva, 115, 19–123 (in Russian; not seen, extracted from Chemical Abstracts, 105-9357r, 1986).

Taylor, A.M., and Terrell, B.C. (1967) Synthetic tourmalines containing elements of the first transition series. Journal of Crystal Growth, 1, 238–244.

Thompson, J.B., Jr. (1979) The Tschermak substitution and reactions in pelitic schists. In V.A. Zharikov, W.I. Fonarev, and S.P. Korikovskiy, Eds., Problems in physico-chemical petrology, vol. 1, p. 146–159. "Nauka" Press, Moscow (in Russian).

——— (1981) An introduction to the mineralogy and petrology of the biopyriboles. Mineralogical Society of America Reviews in Mineralogy, 9A, 141–188.

——— (1982) Composition space: An algebraic and geometric approach. Mineralogical Society of America Reviews in Mineralogy, 10, 1–31.

Tomisaka, T. (1968) Synthesis of some end members of the tourmaline group. Mineralogical Journal (Japan), 5, 355–364.

Velde, B. (1973) Phase equilibria in the system MgO-Al_2O_3-SiO_2-H_2O: Chlorite and associated minerals. Mineralogical Magazine, 39, 297–312.

Werding, G., and Schreyer, W. (1984) Alkali-free tourmaline in the system MgO-Al_2O_3-B_2O_3-SiO_2-H_2O. Geochimica et Cosmochimica Acta, 48, 1331–1344.

Wones, D.R., and Eugster, H.P. (1965) Stability of biotite: Experiment, theory, and applications. American Mineralogist, 50, 1228–1272.

Manuscript received July 1, 1988
Manuscript accepted March 21, 1989